PPPL--2366

DE86 015516

AN EMPIRICAL PARTICLE TRANSPORT MODEL FOR TOKAMAKS

BY

M. PETRAVIC AND G. KUO-PETRAVIC

AUGUST 1986

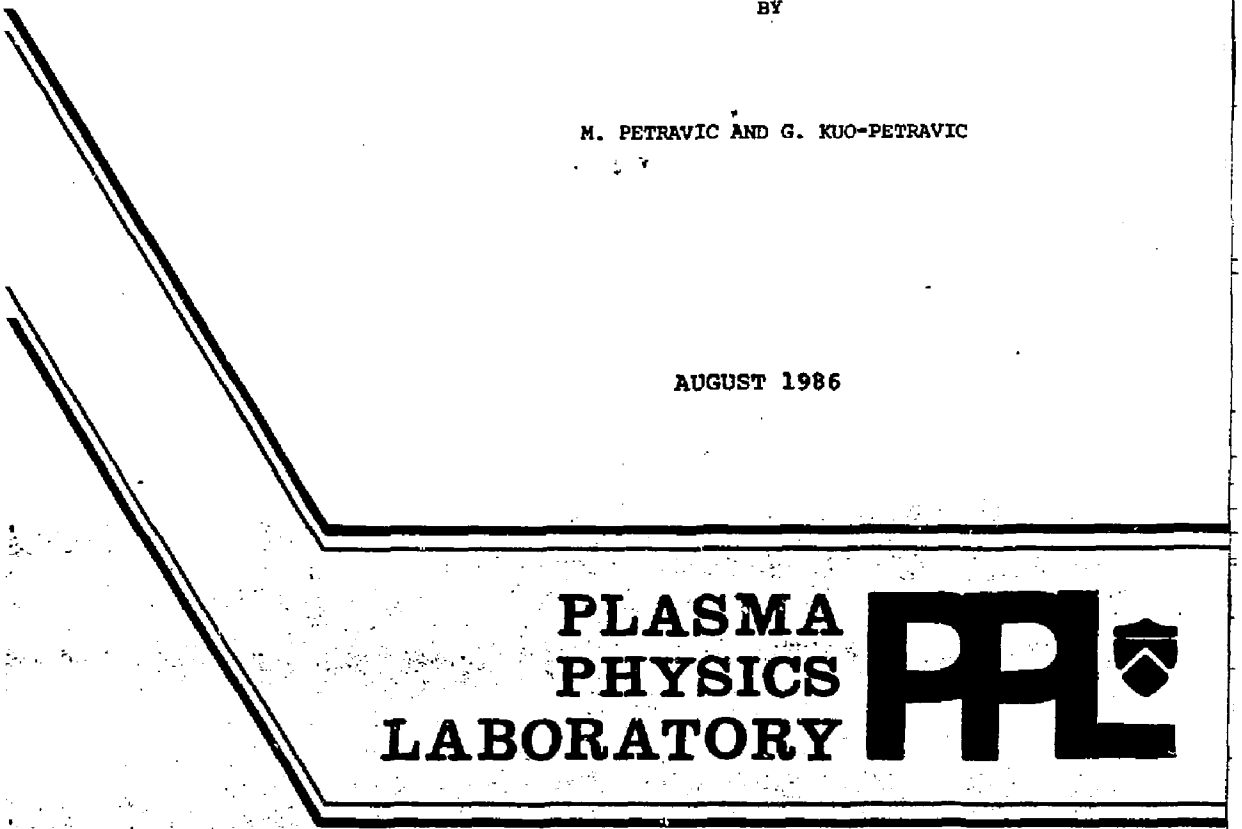

PRINCETON UNIVERSITY
PRINCETON, NEW JERSEY

PREPARED FOR THE U.S. DEPARTMENT OF ENERGY,
UNDER CONTRACT DE-AC02-76-CHO-3073.

NOTICE

Printed in the United States of America

Available from:

National Technical Information Service
U.S. Department of Commerce
5285 Port Royal Road
Springfield, Virginia 22161

Price Printed Copy $ * ; Microfiche $4.50

*Pages	NTIS Selling Price
1-25	$7.00
25-50	$8.50
51-75	$10.00
76-100	$11.50
101-125	$13.00
126-150	$14.50
151-175	$16.00
176-200	$17.50
201-225	$19.00
226-250	$20.50
251-275	$22.00
276-300	$23.50
301-325	$25.00
326-350	$26.50
351-375	$28.00
376-400	$29.50
401-425	$31.00
426-450	$32.50
451-475	$34.00
476-500	$35.50
500-525	$37.00
526-550	$38.50
551-575	$40.00
567-600	$41.50

For documents over 600 pages, add $1.50 for each additional 25-page increment.

AN EMPIRICAL PARTICLE TRANSPORT MODEL FOR TOKAMAKS

M. Petravic and G. Kuo-Petravic

Plasma Physics Laboratory, Princeton University

Princeton, NJ 08544

Abstract

A simple empirical particle transport model has been constructed with the purpose of gaining insight into the L- to H-mode transition in tokamaks. The aim was to construct the simplest possible model which would reproduce the measured density profiles in the L-regime, and also produce a qualitatively correct transition to the H-regime without having to assume a completely different transport mode for the bulk of the plasma. Rather than using completely ad hoc constructions for the particle diffusion coefficient, we assume $D = 1/5\ \chi_{total}$, where $\chi_{total} \approx \chi_e$ is the thermal diffusivity, and then use the $\kappa_e = n_e \chi_e$ values derived from experiments. The observed temperature profiles are then automatically reproduced, but nontrivially, the correct density profiles are also obtained, for realistic fueling rates and profiles. Our conclusion is that it is sufficient to reduce the transport coefficients within a few centimeters of the surface to produce the H-mode behavior. An additional simple assumption, concerning the particle mean-free path, leads to a convective transport term which reverses sign a few centimeters inside the surface, as required by the H-mode density profiles.

Introduction

The L- to H-mode transition in the beam-heated tokamaks has been shrouded in mystery for a number of years. The fact that a change from a limiter to a divertor, both of which are in contact only with the plasma surface, can affect transport properties of the bulk of the plasma was regarded as particularly puzzling. It seemed that two completely different transport regimes were required to explain the phenomenon.

Not less mysterious, though less sensational, is tokamak particle transport in general. The gas fueling produces ions only within the plasma edge, and yet the density profiles exhibit gradients much deeper into the plasma. For the lack of a better prescription, the major transport codes often use a constant diffusion coefficient D, and then add the so-called "anomalous pinch" terms which produce inward mass transport.

Though a simple relationship between the particle transport coefficient D, and the thermal diffusivity χ need not exist, there is also no reason for seeking the most complicated relationship between the two, which is implied in the assumptions like D=constant. The radial dependence of χ_e is admittedly not properly understood, but it is at least not unreasonable to find that it peaks near and beyond the q=2 rational surface. Given that fact, it seems unreasonable to expect that D is constant as a function of radius, an assumption that is often made, since that is regarded as a simple assumption. We would to the contrary argue that a constant D is, in fact, a rather fanciful assumption, in view of the fact that most of the small scale turbulence occurs near the surface, and χ_e increases rapidly with (minor) radius. There appears to be enough experimental evidence indicating a strong correlation between χ_e and D, in auxiliary-heated tokamaks, and a simple relationship $D = 1/5\ \chi_e$ seems to be the most natural choice. In the final

instance, since no reliable theory exists, only a comparison with experiments can show which assumption for D is the most reasonable one.

The Diffusion Equation

In order to get the best possible use of the $D \sim \chi$ assumption, we have to write the diffusion equation in a particular form. Here we follow Braginskii [1] in defining the diffusive particle flux Γ in the positive (Γ^+), and the negative (Γ^-) directions. However, rather than just Taylor-expanding the density as in Eq. (3.1) Ref. 1, we also expand the diffusion speed $v = \Delta r/\tau$, where Δr is the mean-free path, and τ is the corresponding collision time. In our application v is best interpreted as the gyrocenter drift speed in the turbulent $\vec{E} \times \vec{B}$ field. Having expanded both n and v, we get

$$\Gamma^+_{(r)} = \frac{1}{2}\left[n(r) - \frac{dn(r)}{dr}\frac{\Delta r(r)}{2}\right] \times \left[v(r) - \frac{dv(r)}{dr}\frac{\Delta r(r)}{2}\right], \tag{1}$$

$$\Gamma^-_{(r)} = \frac{1}{2}\left[n(r) + \frac{dn(r)}{dr}\frac{\Delta r(r)}{2}\right] \times \left[v(r) + \frac{dv(r)}{dr}\frac{\Delta r(r)}{2}\right]. \tag{2}$$

Subtracting the two equations, we get for $\Gamma = \Gamma^+ - \Gamma^-$, the net diffusive particle flux

$$\Gamma(r) = -\frac{1}{2}\Delta r(r)v(r)\frac{dn(r)}{dr} - \frac{1}{2}\Delta r(r)\frac{dv(r)}{dr}n(r) \quad , \tag{3}$$

where $\Delta r(r)v(r)/2 = D(r)$ is the diffusion coefficient, and $-1/2\Delta r(r)\, dv(r)/dr$ is the convection velocity. The convective term here appears naturally, and is associated with the same diffusion mechanism responsible for D. (This does not preclude the existence of other purely convective transport mechanisms.) We can also write (3) in the form

$$\frac{d}{dr} \ln n(r) + \frac{d}{dr} \ln v(r) = - \frac{\Gamma(r)}{n(r)\ D(r)} \ . \tag{4}$$

Defining the integral

$$I(r) = \int_o^r \frac{\Gamma(r)}{n(r)\ D(r)}\, dr \ , \tag{5}$$

the solution of (4) can be written as

$$n(r) = n(a) \left[\frac{v(a)}{v(r)}\right] \frac{\exp[I(a)]}{\exp[I(r)]} \ , \tag{6}$$

where a is the plasma minor radius. This equation has to be solved simultaneously with the continuity equation $\mathrm{div}(\vec{\Gamma}) = S_n(r)$ which defines $\Gamma(r)$ in terms of the source due to the ionization of the neutral gas surrounding the plasma. Though $S_n(r)$ is a function of $n(r)$, we assume a simple exponential attenuation in all cases. In practice this is a fairly reasonable approximation. $S_n(r)$ is, of course, normalized so that its integral over the whole plasma volume equals the fueling rate. Then

$$\Gamma(r) = \frac{1}{r} \int_o^r S_n(r)\ r dr \tag{7}$$

can be evaluated, and used in Eq. (5). It is seen that in the region where fueling is nonexistent or low, the diffusion speed is simply given by $v(r) = v(a)n(a)/n(r)$, independently of any specific diffusion model.

The Diffusion Model

In constructing the particle diffusion model, we are guided by the

observation that in the PDX experiment the temperature profile in the H-mode could be obtained by putting the L-mode profile onto a 200-250 eV pedestal (Fig. 1). From this we conclude that the following relationship must exist between the diffusivities in the two cases

$$\left[n(r)\chi(r)\right]_H = \left[n(r)\chi(r)\right]_L \; ; \; 0 \leq r \leq r_m \; ,$$

and

$$\left[n(r)\chi(r)\right]_H < \left[n(r)\chi(r)\right]_L \; ; \; r_m < r \leq a,$$

where r_m is the radius, close to a, at which $K(r) = n(r)\chi(r)$ has a maximum. We therefore find it convenient to define the normalized thermal conductivity $K_n(r) = n(r)\chi(r)/[n(r_m)\chi(r_m)]$ which has a maximum value of 1 at $r = r_m$. From the fact that within the operating range under consideration, and for $0 \leq r \leq r_m$, $n(r)$ changes between the two modes, while $n(r)\chi(r)$ does not, we conclude that $\chi \sim 1/n$. We shall make use of the latter inverse dependence on n, but our model does not depend on it in an essential way, only the computation is simplified. The model itself is defined by the following three relationships:

$$D = \frac{\Delta r(r) v(r)}{2} = \frac{1}{5}\chi = \frac{1}{5}\frac{K(r)}{n(r)} \; , \tag{8}$$

$$\Delta r(r) = \frac{\Delta r_o n(r_m)}{n(r)} K_n^{1-s}(r) \; , \tag{9}$$

and

$$v(r) = v_m K_n^s(r) \; , \tag{10}$$

where Δr_o, v_m, and $n(r_m)$ are constants. Since these constants will appear only in the product $\Delta r_o v_m n(r_m)$, it is useful to define

$$c_m = \Delta r_o v_m n(r_m) = \frac{1}{5} \chi(r_m)\, n(r_m) \ . \tag{11}$$

The exponent s in (9) and (10) is a free parameter and will be discussed later. Using the model definition (8), (9), (10), and (11), we can write the solution (6) in the form

$$n(r) = n(a) \left[\frac{K_n(a)}{K_n(r)}\right]^s \frac{\exp[I(a)]}{\exp[I(r)]} \ , \tag{12}$$

where now

$$I(r) = \frac{1}{c_m} \int_o^r \frac{\Gamma(r)}{K_n(r)}\, dr. \tag{13}$$

Since I(0) = 0, we also have for the central density

$$n(0) = n(a) \left[\frac{K_n(a)}{K_n(0)}\right]^s \exp\left[I(a)\right] \ . \tag{14}$$

For the diffusive energy transport, we use a simple equation with only the conduction term

$$\frac{1}{r}\frac{d}{dr}\left(r\, K(r)\, \frac{dT}{dr}\right) = P(r) \ , \tag{15}$$

where P(r) is the deposited power per unit volume.

Results

In computing solutions for the model, it would be desirable to use an experimentally determined K(r). However, what is more readily available is

$\chi_e(r)$ derived from experimental temperature profiles, using some transport model. For that reason and as a first step, we construct $K_n(r)$ from two Gaussian functions joined at their maximum, and then compare the result directly with the temperature profiles, and the $\chi_e(r)$ from other transport analysis. Since our $K_n(r)$ is chosen to fit the experimental results, it has to be regarded as derived from the experiment using our simple energy transport model. It should also be mentioned that although our power deposition profiles are not very accurate, the result is not very sensitive to these profiles.

The real test of the model comes in the prediction of the density profiles. However, we have to mention at the outset that no extensive comparison with the measurements has been made so far, and that such comparisons would be done best by incorporating the model into a code which treats the power and particle deposition self-consistently, computes other energy loss mechanisms, and takes account of the Shafranov shift, etc. We therefore seek here a good qualitative, and only a moderate quantitative agreement with experiments. In particular, we compare the model results with the PDX results of Fonck et al. [2].

Strictly, there is only one free parameter in the model, the exponent s of $K_n(r)$ in Eqs. (9) and (10), assuming K(r) is given. This parameter determines how much of the K dependence on r is due to the variation in $\Delta r(r)$, and how much due to v(r). We used $s = 1/2$, but values of s up to s=1 are not ruled out. In practice, n(a) is not a very well-known quantity, since the minor radius a is not known to better than ± 1 cm. Also, since the neutral gas injection in the relevant PDX experiment was into the divertor chamber, the equivalent fueling rate is not accurately known. For all the above reasons the modeling parameters were as follows: radius of the K_{max}, r_m = 35

cm, minor radius a = 40 cm, major radius R = 140 cm (for computing the volume), total input power P_{tot} = 1.5 MW, and the plasma density at a n(a) = 2 × $10^{12}/cm^3$. Of the remaining parameters the gas injection rate was varied between 10 torr ℓ/sec and 20 torr ℓ/sec, with a fixed deposition profile $S_n = S_o \exp[-(a-r)/4]$. As described earlier, K(r) was chosen so as to reproduce the electron temperature profiles of Fig. 1, Ref. 2. In particular, the same $K_n(r)$, $0 \leq r \leq r_m$, was used for both the L- and the H-mode. To reproduce the temperature pedestal in the H-mode, $K_n(r)$ was reduced in the region $r_m < r \leq a$. The radial dependencies of $K_n(r)$ are shown in Fig. 2. The corresponding diffusivities $\chi(r)$ are shown in Fig. 3. The temperature profiles in Fig. 4 exhibit the characteristic H-mode pedestal of roughly the observed magnitude. The really important fact is that now the density profiles also have the correct shape, with a very marked pedestal in the H-mode. The H-mode solution in Fig. 5 was produced with a fueling rate of 12 torr ℓ/sec, while the L-mode requires 18 torr ℓ/sec. If the same rate of 12 torr ℓ/sec is used in both cases, the L-mode density is much lower, as shown in Fig. 6.

The remaining figures provide quantities relevant for comparison with the standard particle transport model. They show the diffusion coefficient (Fig. 7), convection velocity (Fig. 8), and the diffusive and convective fluxes for the L-mode (Fig. 9), and the H-mode (Fig. 10). The outward convective transport, essential in the H-mode, again results naturally from the decrease in K/a. Finally, we show the mean-free path $\Delta r(r)$ in Fig. 11, and the diffusion speed v(r) in Fig. 12.

The diffusion coefficient and the convective velocity show a second peak very close to r = a. This is dus to the very low value of n(a), which probably already belongs to the scrapeoff. As a consequence, our radial diffusion model is then trying to do the work of the large parallel transport

in the scrape-off region.

Summary

A particle transport model has been constructed which assumes a close link between the particle diffusion coefficient D and the thermal diffusivity χ by setting $D(r) = 1/5\ \chi(r)$. Furthermore, the convection term was written in a form which enabled us to identify it as made up of the factors of $D = (\Delta r)^2/\tau$, namely, Δr and $v = \Delta r/\tau$. This made it possible to guess at the relationship of Δr, v, and $K(r) = n(r)\chi(r)$. The result was a particle transport equation encompassing both diffusion and convection which permits a zero net particle flux in the presence of density gradients. This equation qualitatively correctly reproduces the standard L-mode density profiles, and even quantitatively it appears capable of reproducing the measured values. As far as the H-mode is concerned, it very strongly suggests that the improvement in both the global energy and particle confinement is due to a reduction of diffusion in only a few cm of the edge just inside the separatrix. This, of course, does not explain the mechanism, but it localizes the cause. The beneficial effect spreads to the inside through the increase of the particle density, and through the related lowering of χ ($\chi \sim 1/n$). Therefore, no qualitatively different transport mechanisms are required in this case for the bulk of the plasma. (There is no sawtooth model, so if there is a difference in the L- and H-mode sawteeth, it will not be borne out). In a higher density, temperature, or a higher injected power regime, the $\chi \sim 1/n$ dependence may not exist, but that does not affect the essential part of the model, only the H-mode will be less good.

It seems to us that the assumption $D \sim \chi$, if it survives more comparisons with experiments, is likely to hold out in other regimes as well, and

maintain the usefulness of the model. Here, $D \sim \chi$ is not meant as an exact relationship, it really only implies that the two are likely to be closely related rather than being independent quantities. While the correctness and usefulness of any empirical model depends solely on how well it agrees with the experimental facts, our model has a number of interesting mathematical features which may help to identify the crucial features in the experiments. To start with, the sign of the second term in (3) changes at $r = r_m$, which permits positive density gradients between r_m and the edge, and not just a flat pedestal. Without a positive density gradient there is no inward diffusive transport beyond $r = r_m$. There are implications here for impurity transport.

Another interesting feature is the exponential factor in (12). For large $K_m(r)$ and small $\Gamma(r)$, $I(r) < I(a) << 1$, and we get an "ideal" L-mode: $n(r) = n(a)\ [K_m(a)/K_m(r)]^{1/2}$. The density amplification factor from the surface to the center is simply $[K_m(a)/K_m(0)]^{1/2}$. We are not aware of such a mode being observed and find that a more typical L-mode has $I(a) \approx 1$, providing additional amplification of ~ 3. Due to the same exponential factor the H-mode sets in very suddenly for $I(a) > 1$. The largest increase in $I(r)$ occurs very close to $r = a$, due to the drop in $K_m(r)$ [see Eq. (13)], hence, the steep drop in $n(r)$ at $r \approx a$, creating a pedestal. The height of the pedestal also depends on the magnitude of $K(r_m)$, which was here kept constant, but is probably somewhat reduced in reality, raising the pedestal even further. Finally, it is hoped that the insight provided by the presented results will encourage the search for the actual cause of the reduction of diffusion near the separatrix.

Acknowledgments

We would like to thank R. J. Fonck and the PDX team for allowing us to reproduce their results in Fig. 1, and M. Redi for the helpful discussion and encouragement.

This work was supported by the U.S. Department of Energy Contract No. DE-AC02-76-CHO-3073.

References

[1] S. I. Braginskii, Rev. Plasma Phys. 1 (1965) 205.

[2] R. J. Fonck *et al.*, Fourth International Symposium on Heating in Toroidal Plasmas, Rome, March 21, 1984; Princeton Plasma Physics Laboratory Report No. PPPL-2118 (1984).

Figure Captions

FIG. 1. Electron temperature and density profiles from Thomson scattering for the L- and H-mode phases of a high confinement discharge, from R. Fonck et al. [2].

FIG. 2. Normalized thermal conductivity as a function of the minor radius for the L-mode (dashed curve), and the H-mode (full curve).

FIG. 3. The electron thermal diffusivity χ for the L (dashed curve) and the H-mode (full curve), corresponding to the conductivities K of Fig. 2.

FIG. 4. The electron temperature profiles for the L- and H-modes, the latter exhibiting the characteristic pedestal, for 1.5 MW of transported power.

FIG. 5. The electron density profiles for the low- and high-confinement modes correspond to the fueling rates of 18 torr-liters/sec and 12 torr liters/sec, respectively.

FIG. 6. The electron density profiles for the low- and high-confinement modes for the fueling rate of 12 torr liters/sec.

FIG. 7. Particle diffusion coefficients for the low (L) and high (H) confinement modes. For $r \leq r_m = 35$ cm, the two are related by $D_H(r)$ $\eta_H(r) = D_L(r)$ $\eta_L(r)$.

FIG. 8. Convection velocity is almost equal for the two modes except for the outer 3 cm of the edge. The very high values of V_{conv} within the first 1 cm of the radius are probably due to assigning a too low density value at $r = a$, a value that most likely belongs to the scrapeoff. The same applies to the transport coefficients of Fig. 7.

FIG. 9. Diffusive and convective components of the L-mode particle flux. Beyond $r \approx 25$ cm, the diffusive flux dominates.

FIG. 10. Diffusive and convective parts of the H-mode particle flux. The outward convection carries the whole of the flux in the plato region.

FIG. 11. The mean-free path $\Delta r(r)$ for the L- and H-modes.

FIG. 12. Diffusion speed $v(r)$ as a function of radius.

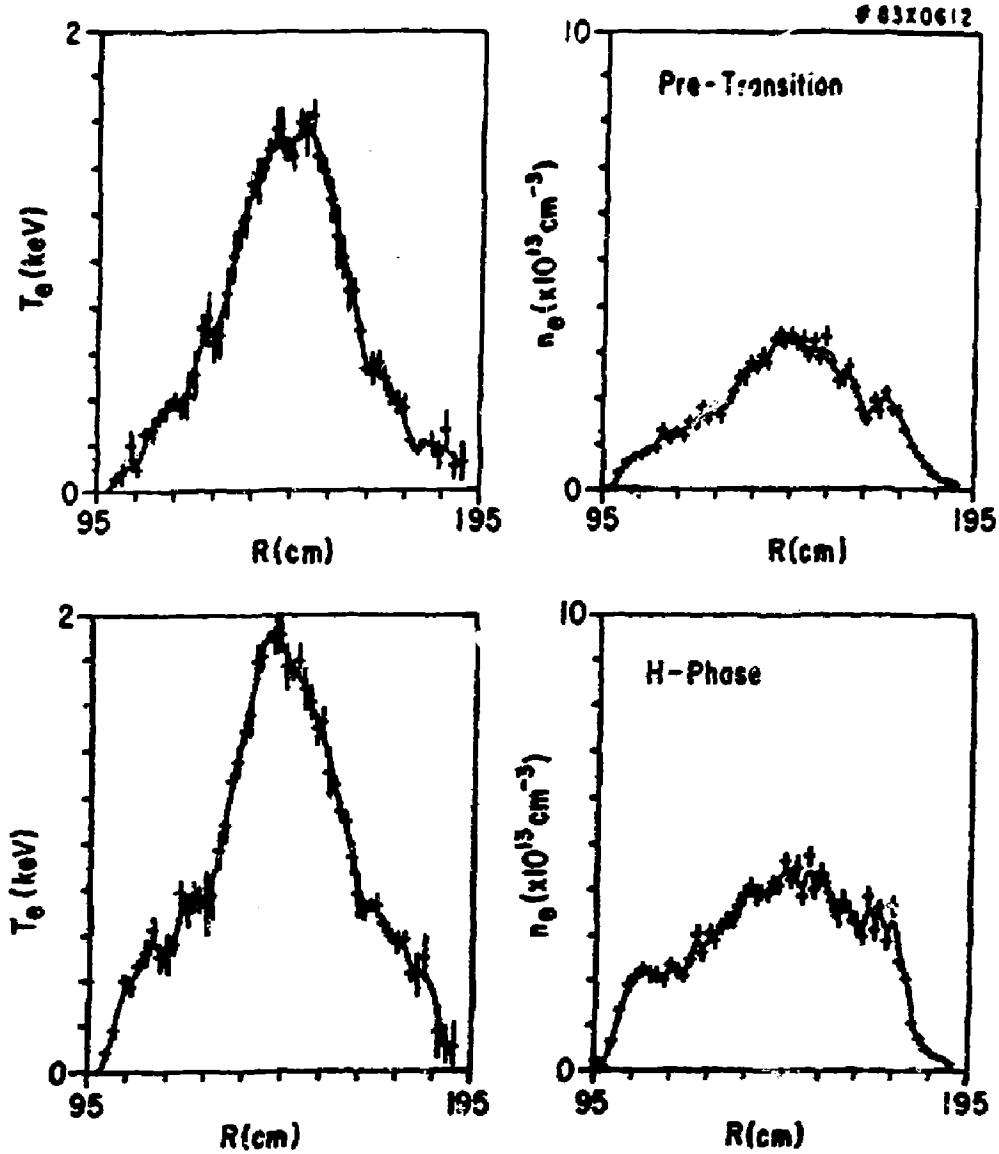
#83X0612
Pre-Transition
H-Phase
T_e (keV)
n_e ($\times 10^{13}$ cm^{-3})
R(cm)
0
2
10
95
195

FIG. 1

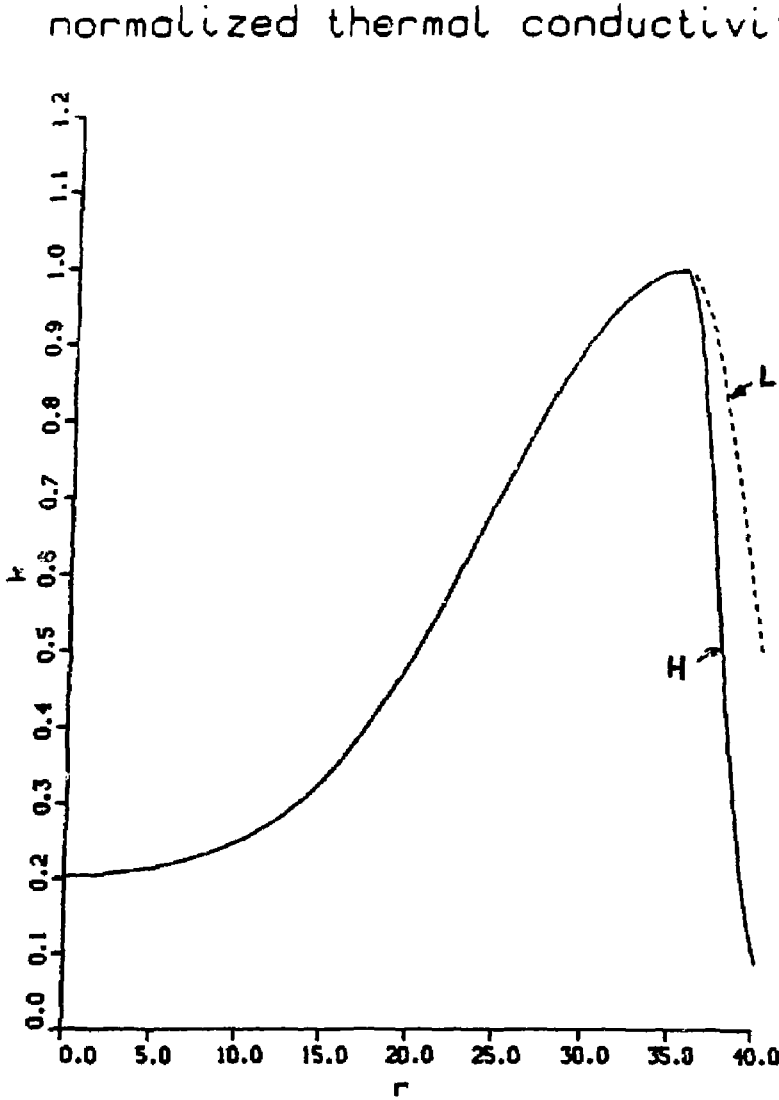
normalized thermal conductivity
k
r
L
H
0.0
0.1
0.2
0.3
0.4
0.5
0.6
0.7
0.8
0.9
1.0
1.1
1.2
0.0
5.0
10.0
15.0
20.0
25.0
30.0
35.0
40.0

FIG. 2

DIFFUSIVITY

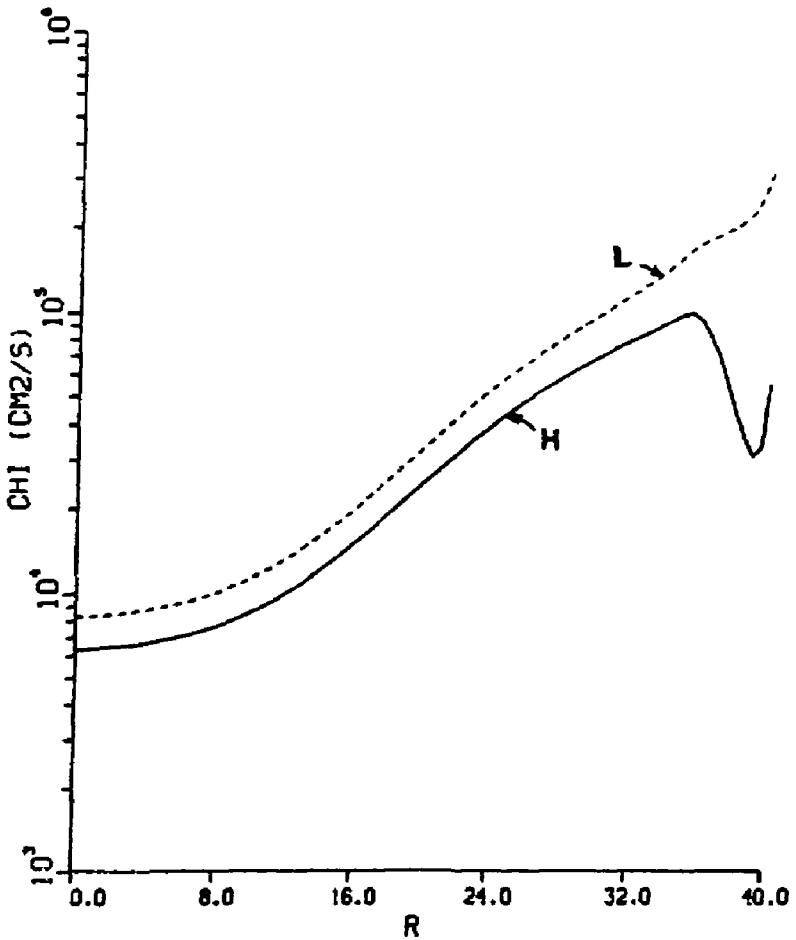

FIG. 3

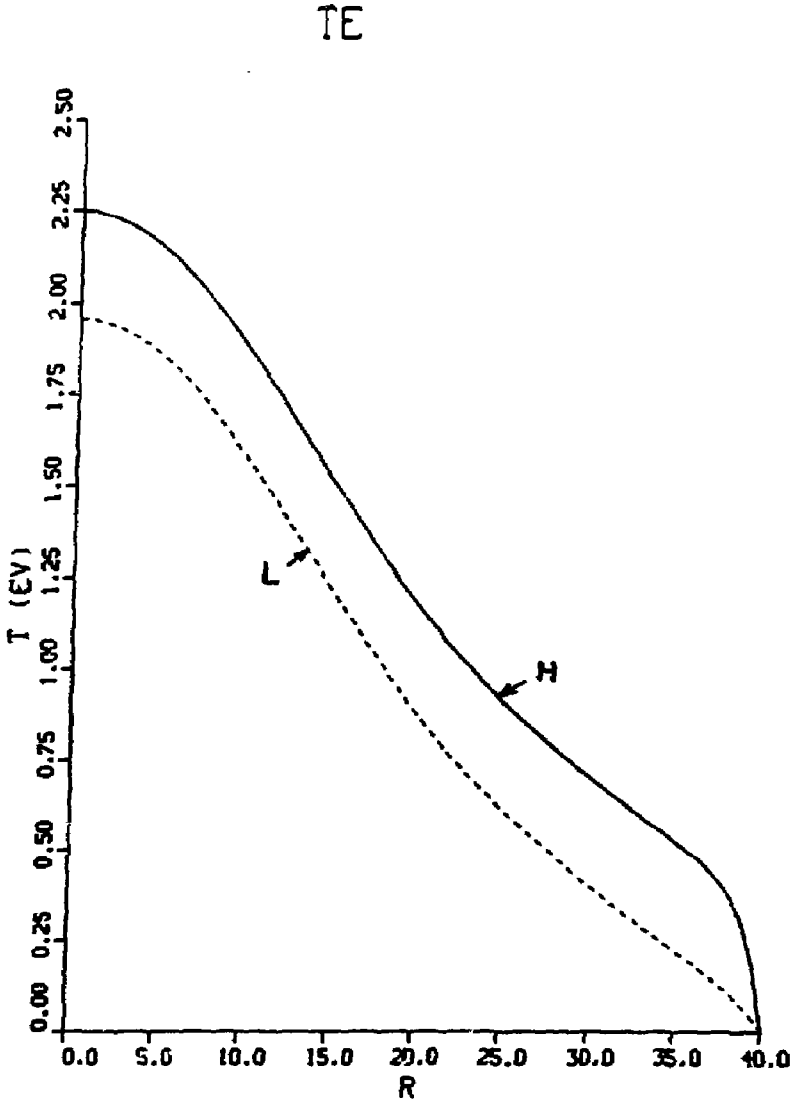
TE
T (EV)
0.00
0.25
0.50
0.75
1.00
1.25
1.50
1.75
2.00
2.25
2.50
L
H
0.0
5.0
10.0
15.0
20.0
25.0
30.0
35.0
40.0
R

FIG. 4

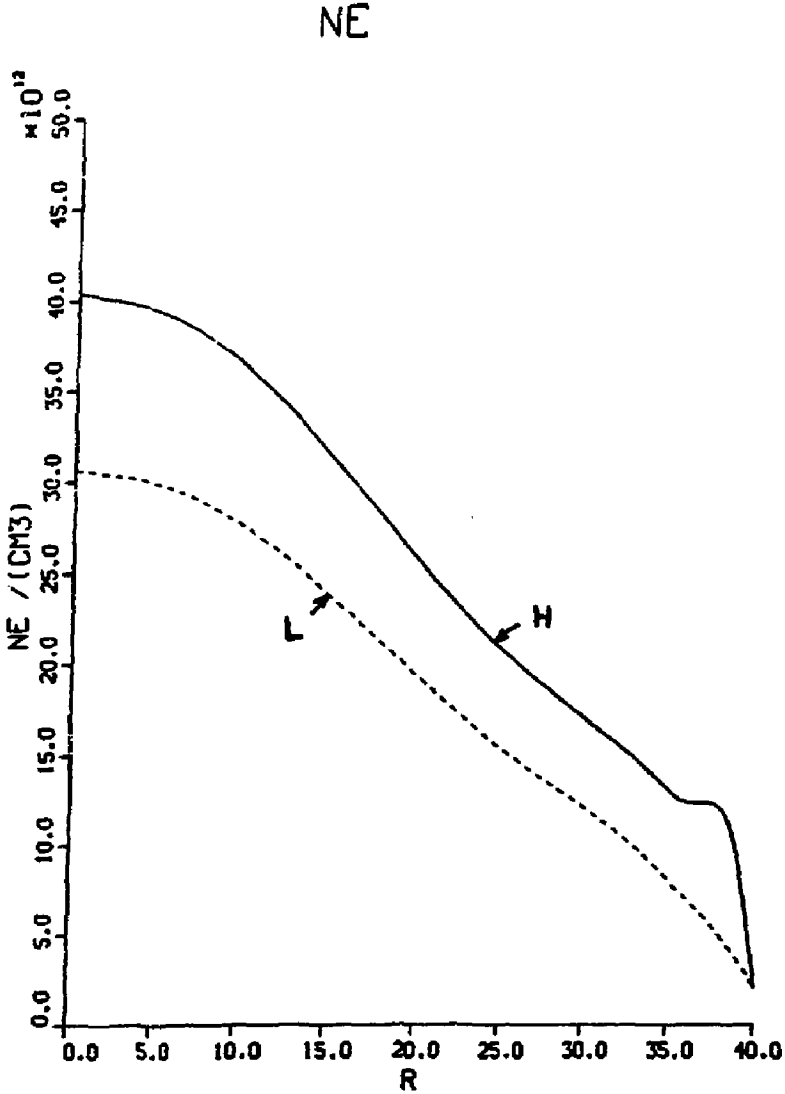
NE
NE /(CM3)
×10¹²
50.0
45.0
40.0
35.0
30.0
25.0
20.0
15.0
10.0
5.0
0.0
L
H
0.0
5.0
10.0
15.0
20.0
25.0
30.0
35.0
40.0
R

FIG. 5

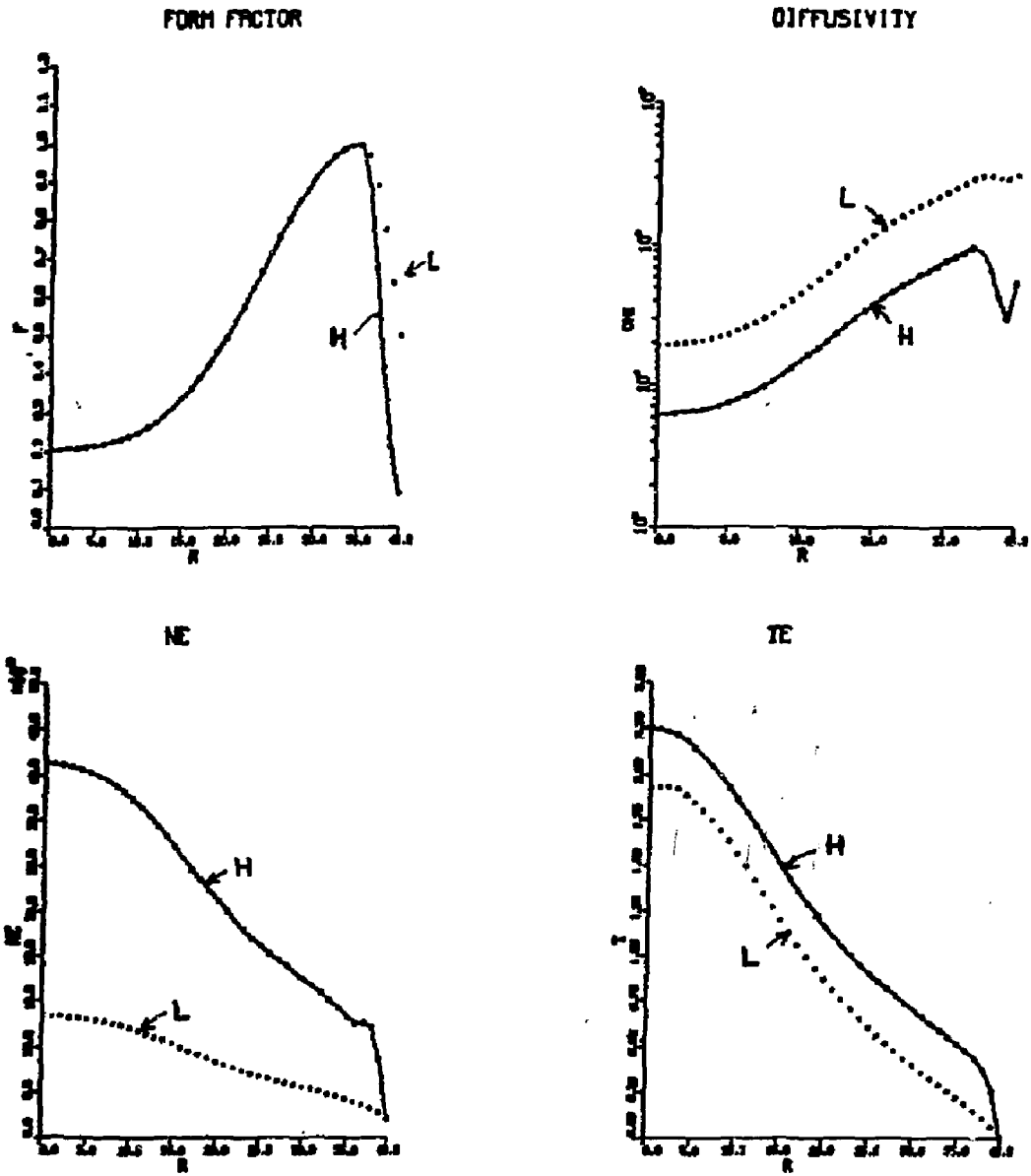

FIG. 6

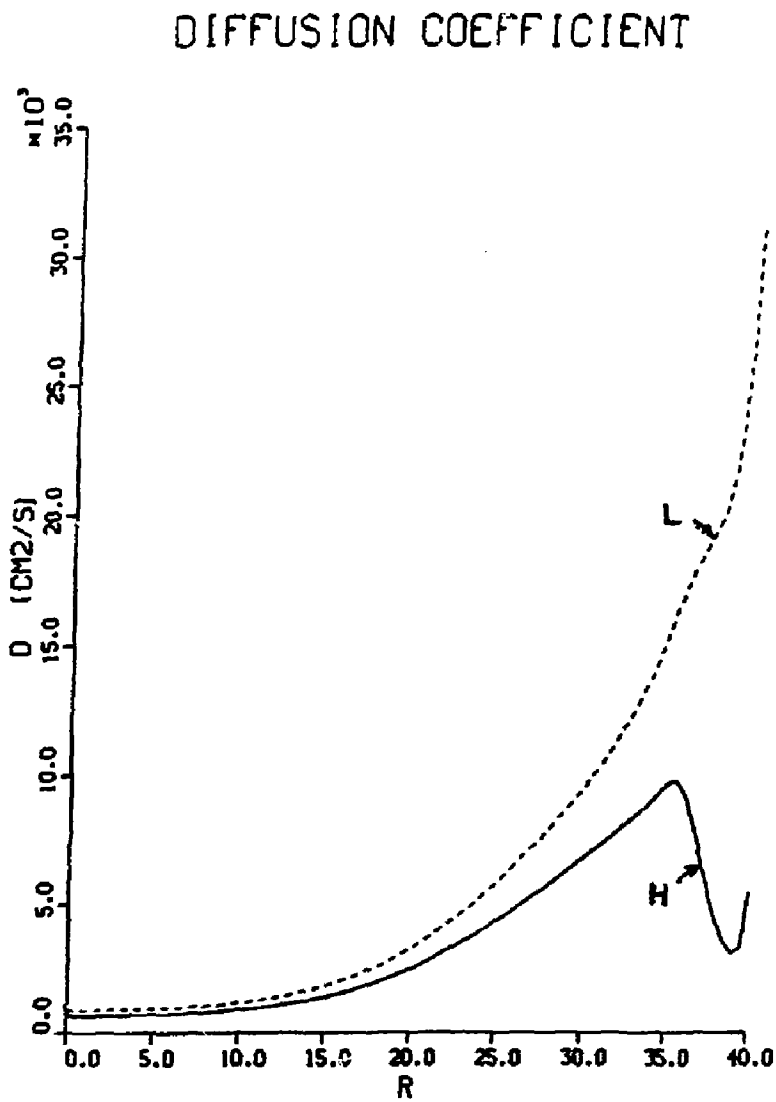
DIFFUSION COEFFICIENT
D (CM2/S) ×10³
35.0
30.0
25.0
20.0
15.0
10.0
5.0
0.0
L
H
0.0
5.0
10.0
15.0
20.0
25.0
30.0
35.0
40.0
R

FIG. 7

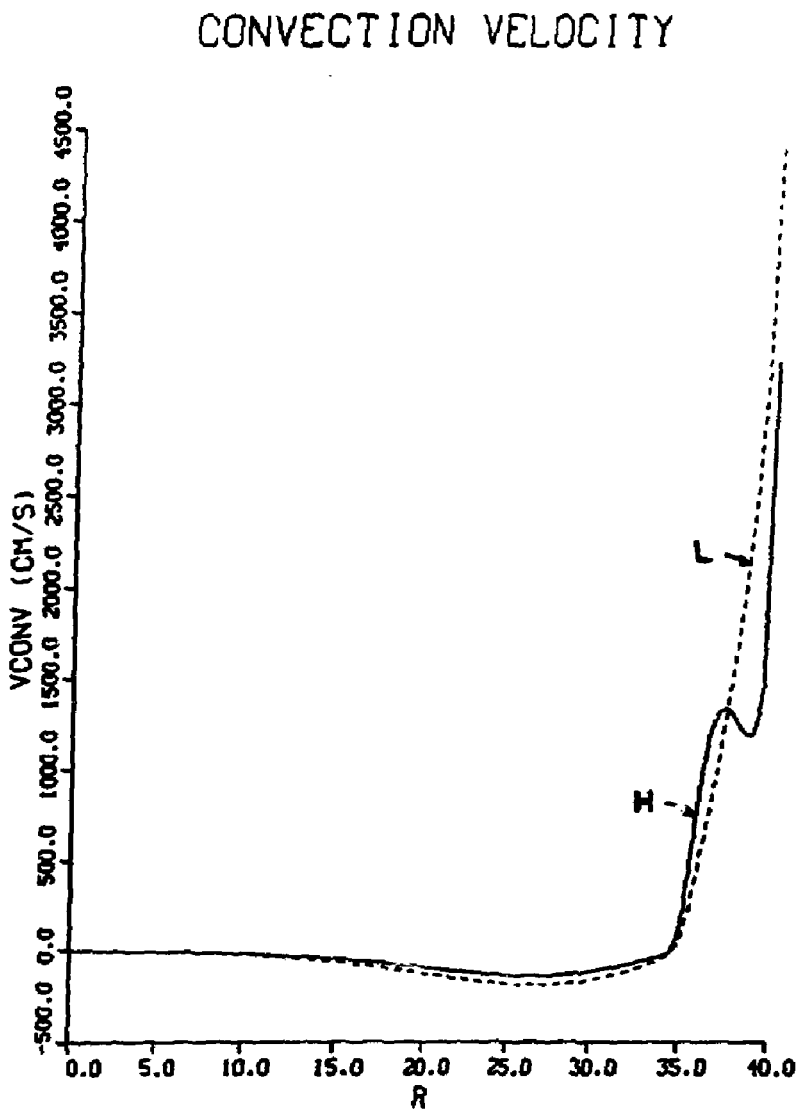
CONVECTION VELOCITY
VCONV (CM/S)
-500.0
0.0
500.0
1000.0
1500.0
2000.0
2500.0
3000.0
3500.0
4000.0
4500.0
0.0
5.0
10.0
15.0
20.0
25.0
30.0
35.0
40.0
R
L
H

FIG. 8

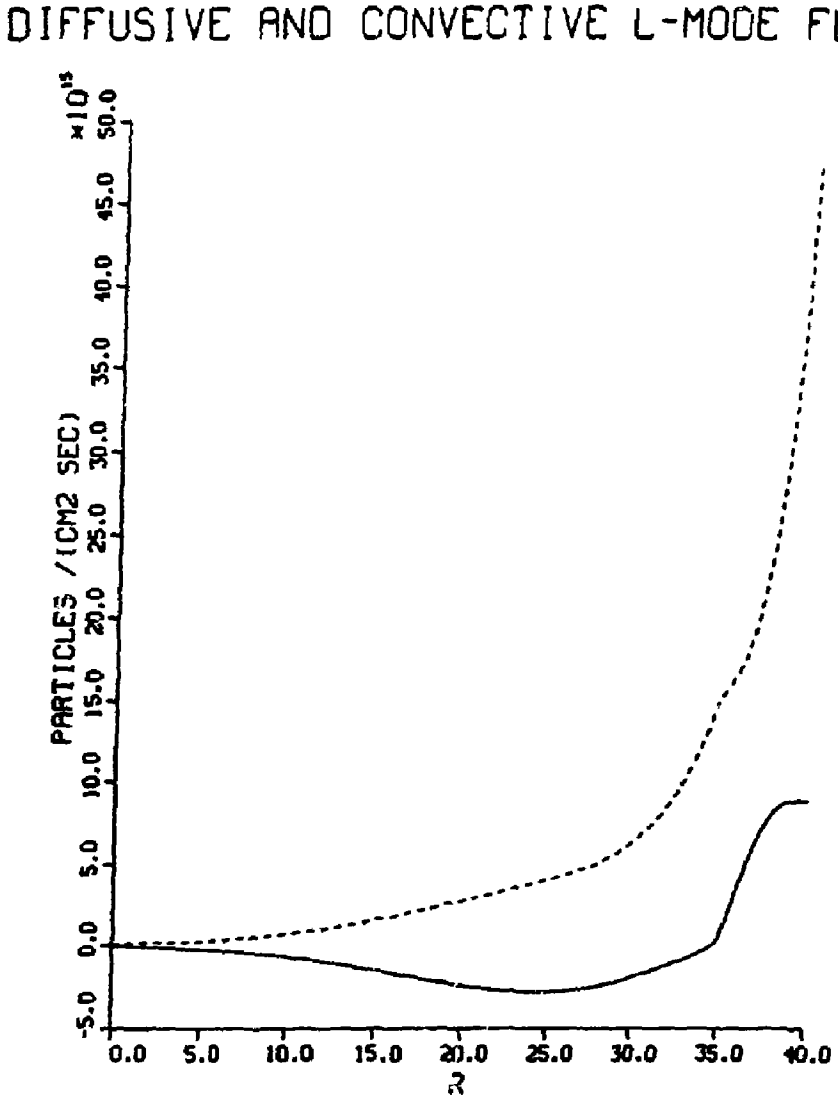
DIFFUSIVE AND CONVECTIVE L-MODE FLUXES
PARTICLES /(CM2 SEC)
×10^18
50.0
45.0
40.0
35.0
30.0
25.0
20.0
15.0
10.0
5.0
0.0
-5.0
0.0
5.0
10.0
15.0
20.0
25.0
30.0
35.0
40.0
R

FIG. 9

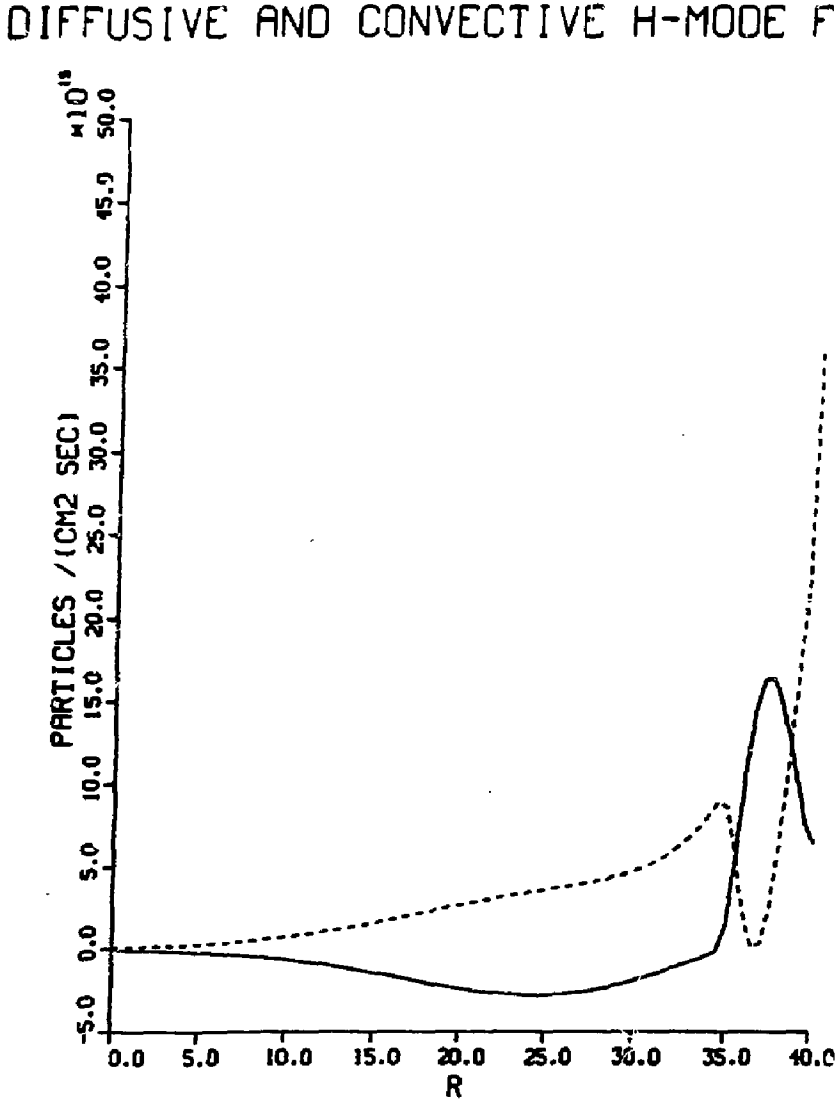
DIFFUSIVE AND CONVECTIVE H-MODE FLUXES
PARTICLES /(CM2 SEC)
*10**18
50.0
45.0
40.0
35.0
30.0
25.0
20.0
15.0
10.0
5.0
0.0
-5.0
0.0
5.0
10.0
15.0
20.0
25.0
30.0
35.0
40.0
R

FIG. 10

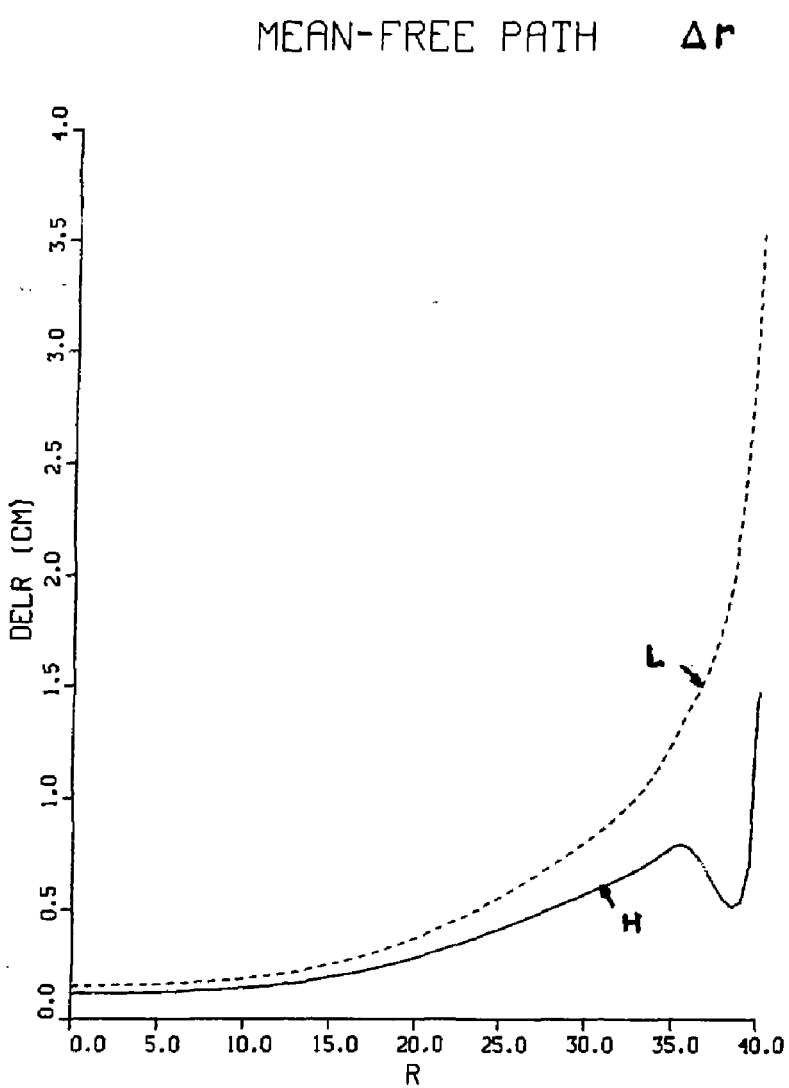
MEAN-FREE PATH Δr
DELR (CM)
0.0
0.5
1.0
1.5
2.0
2.5
3.0
3.5
4.0
0.0
5.0
10.0
15.0
20.0
25.0
30.0
35.0
40.0
R
L
H

FIG. 11

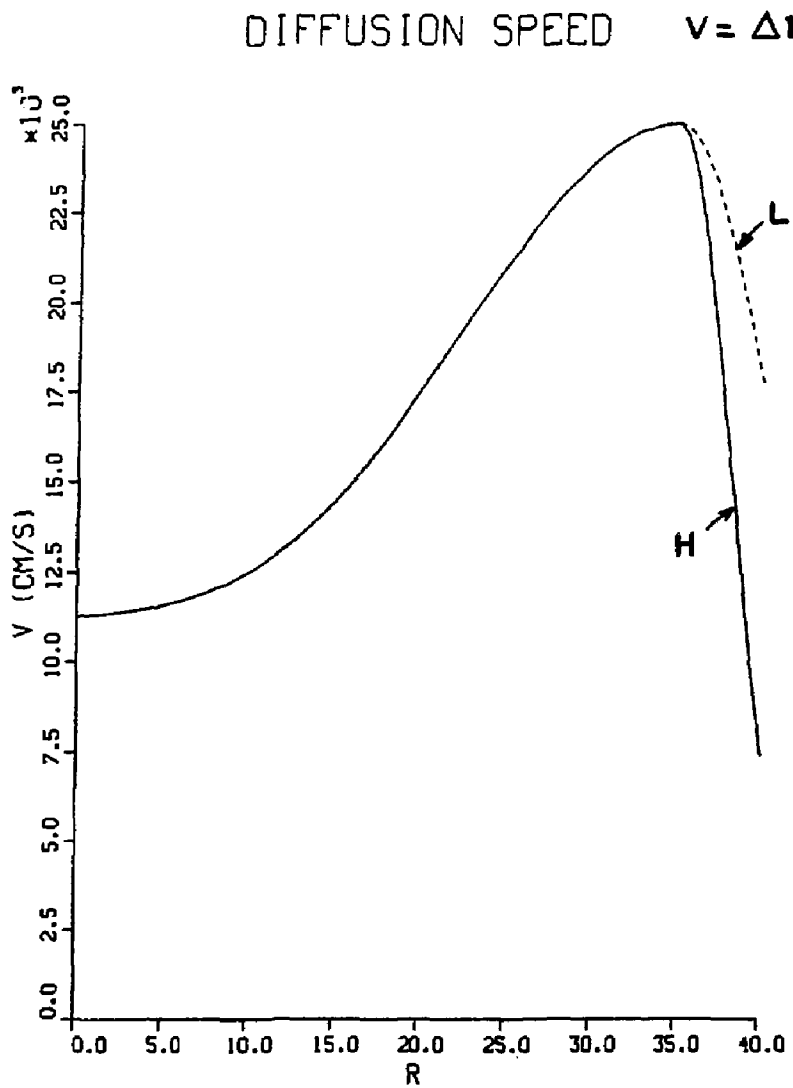
DIFFUSION SPEED $V = \Delta r/\tau$
V (CM/S)
×10³
0.0
2.5
5.0
7.5
10.0
12.5
15.0
17.5
20.0
22.5
25.0
0.0
5.0
10.0
15.0
20.0
25.0
30.0
35.0
40.0
R
L
H

FIG. 12

EXTERNAL DISTRIBUTION IN ADDITION TO UC-20

Plasma Res Lab, Austra Nat'l Univ, AUSTRALIA
Dr. Frank J. Paoloni, Univ of Wollongong, AUSTRALIA
Prof. I.R. Jones, Flinders Univ., AUSTRALIA
Prof. M.H. Brennan, Univ Sydney, AUSTRALIA
Prof. F. Cap, Inst Theo Phys, AUSTRIA
M. Goossens, Astronomisch Instituut, BELGIUM
Prof. R. Boucique, Laboratorium voor Natuurkunde, BELGIUM
Dr. D. Palumbo, Dg XII Fusion Prog, BELGIUM
Ecole Royale Militaire, Lab de Phys Plasmas, BELGIUM
Dr. P.H. Sakanaka, Univ Estadual, BRAZIL
Lib. & Doc. Div., Instituto de Pesquisas Espaciais, BRAZIL
Dr. C.R. James, Univ of Alberta, CANADA
Prof. J. Teichmann, Univ of Montreal, CANADA
Dr. H.M. Skarsgard, Univ of Saskatchewan, CANADA
Prof. S.R. Sreenivasan, University of Calgary, CANADA
Prof. Tudor W. Johnston, INRS-Energie, CANADA
Dr. Hannes Barnard, Univ British Columbia, CANADA
Dr. M.P. Bachynski, MPB Technologies, Inc., CANADA
Chalk River, Nucl Lab, CANADA
Zhengwu Li, SW Inst Physics, CHINA
Library, Tsing Hua University, CHINA
Librarian, Institute of Physics, CHINA
Inst Plasma Phys, Academia Sinica, CHINA
Dr. Peter Lukac, Komenskeho Univ, CZECHOSLOVAKIA
The Librarian, Culham Laboratory, ENGLAND
Prof. Schatzman, Observatoire de Nice, FRANCE
J. Radet, CEN-BP6, FRANCE
JET Reading Room, JET Joint Undertaking, ENGLAND
AM Dupas Library, AM Dupas Library, FRANCE
Dr. Tom Muai, Academy Bibliographic, HONG KONG
Preprint Library, Cent Res Inst Phys, HUNGARY
Dr. R.K. Chhajlani, Vikram Univ, INDIA
Dr. B. Dasgupta, Saha Inst, INDIA
Dr. P. Kaw, Physical Research Lab, INDIA
Dr. Phillip Rosenau, Israel Inst Tech, ISRAEL
Prof. S. Cuperman, Tel Aviv University, ISRAEL
Prof. G. Rostagni, Univ Di Padova, ITALY
Librarian, Int'l Ctr Theo Phys, ITALY
Miss Clelia De Palo, Assoc EURATOM-ENEA, ITALY
Biblioteca, del CNR EURATOM, ITALY
Dr. H. Yamato, Toshiba Res & Dev, JAPAN
Direc. Dept. Lg. Tokamak Dev. JAERI, JAPAN
Prof. Nobuyuki Inoue, University of Tokyo, JAPAN
Research Info Center, Nagoya University, JAPAN
Prof. Kyoji Nishikawa, Univ of Hiroshima, JAPAN
Prof. Sigeru Mori, JAERI, JAPAN
Prof. S. Tanaka, Kyoto University, JAPAN
Library, Kyoto University, JAPAN
Prof. Ichiro Kawakami, Nihon Univ, JAPAN
Prof. Satoshi Itoh, Kyushu University, JAPAN
Dr. D.I. Choi, Adv. Inst Sci & Tech, KOREA
Tech Info Division, KAERI, KOREA
Bibliotheek, Fom-Inst Voor Plasma, NETHERLANDS
Prof. B.S. Liley, University of Waikato, NEW ZEALAND
Prof. J.A.C. Cabral, Inst Superior Tecn, PORTUGAL
Dr. Octavian Petrus, ALI CUZA University, ROMANIA
Prof. M.A. Hellberg, University of Natal, SO AFRICA
Dr. Johan de Villiers, Plasma Physics, Nucor, SO AFRICA
Fusion Div. Library, JEN, SPAIN
Prof. Hans Wilhelmson, Chalmers Univ Tech, SWEDEN
Dr. Lennart Stenflo, University of UMEA, SWEDEN
Library, Royal Inst Tech, SWEDEN
Centre de Recherchesen, Ecole Polytech Fed, SWITZERLAND
Dr. V.T. Tolok, Kharkov Phys Tech Ins, USSR
Dr. D.D. Ryutov, Siberian Acad Sci, USSR
Dr. G.A. Eliseev, Kurchatov Institute, USSR
Dr. V.A. Glukhikh, High Electro-Physical, USSR
Institute Gen. Physics, USSR
Prof. T.J.M. Boyd, Univ College N Wales, WALES
Dr. K. Schindler, Ruhr Universitat, W. GERMANY
ASDEX Reading Rm, IPP/Max-Planck-Institut fur Plasmaphysik, F.R.G.
Nuclear Res Estab, Julich Ltd, W. GERMANY
Librarian, Max-Planck Institut, W. GERMANY
Bibliothek, Inst Plasmaforschung, W. GERMANY
Prof. R.K. Janev, Inst Phys, YUGOSLAVIA